Numerical modeling of cardiovascular physiology Study of dynamic changes during autonomic reflexes and applications to acute myocardial infarction

João Apura
joao.apura@tecnico.ulisboa.pt

Instituto Superior Técnico, Lisboa, Portugal

December 2016

Abstract

Simultaneous pressure and volume measurements enable the extraction of valuable parameters for left ventricle function assessment. The goal of this study was to develop a pressure-volume (PV) computational framework to accurately characterize instantaneous left ventricular (LV) and arterial physiologic properties in rabbits from single-beat parameters, during reflex cardiovascular responses, and how these can be compromised after the acute phase of myocardial infarction.

Reflexes were evoked in fourteen anesthetized, paralyzed and artificially ventilated rabbits, and heart ischemia was provoked by ligation of the descending coronary artery. An intraventricular impedance catheter was used to measure simultaneously LV pressure and volume. The developed software estimated single-beat left ventricle end-systolic elastance (E_{es}), arterial elastance (E_a) and their ratio (E_a/E_{es}) to analyze ventriculo-arterial coupling. From this data, left ventricle stroke work (SW), total energy expenditure (PVA), ratio of the stroke work to its theoretical maximum (Q_{load}) and cardiac energetic efficiency ($CWE = SW/PVA$) were estimated.

E_{es}, E_a, SW and PVA were significantly different between measurements for all cardiovascular reflexes. E_a/E_{es} ratio, Q_{load} and CWE were unaffected between measurements. Acute myocardial infarction contributed to a significant depression in cardiac contractility, augmented cardiac SW and higher oxygen consumption. An unbalanced increase in workload and oxygen consumption resulted in a depression of Q_{load} and CWE. Activation of cardiovascular reflexes in infarcted hearts revealed similar hemodynamic responses as in the control group for E_a, SW and PVA.

These findings indicate the autonomic reflexes revealed a balanced control of induced homeostatic perturbations by simultaneously modeling cardiac contractility, arterial tone and stroke work, in such a way ventriculo-arterial coupling and cardiac efficiency were maintained close to optimal values. Acute myocardial infarction resulted in a deterioration of E_a/E_{es} ratio, Q_{load} and CWE. After heart ischemia, activation of autonomic reflexes revealed that cardiac efficiency and energy transmission to the arterial system were optimized differently according to each reflex.

Keywords: Cardiovascular reflexes, Acute myocardial infarction, Single-beat method, Ventriculo-arterial coupling, Cardiac efficiency

The evaluation of the left ventricle (LV) performance is of high importance in clinical practice and physiologic investigation [Rodriguez et al., 2015]. To characterize LV pump function, volume and pressure signals may be combined to construct pressure-volume (PV) loops **Figure 1**. Each counter-clockwise loop represents one cardiac cycle. The shape and position of the PV loop reflects the interactions between the mechanical properties and the preload and afterload states of the myocardium [Ten Brinke et al., 2010]. A wide variety of indices that can be estimated from pressurevolume (PV) loops have been proposed to characterize LV systolic and diastolic performance, mechanical energies and efficiency.

The end-systolic pressure and volume relationship (ESPVR) is generally accepted as a reliable, sensitive and load-independent measure of the systolic function of the LV. Its slope has been shown to be related to LV contractile state [Burkhoff et al.,

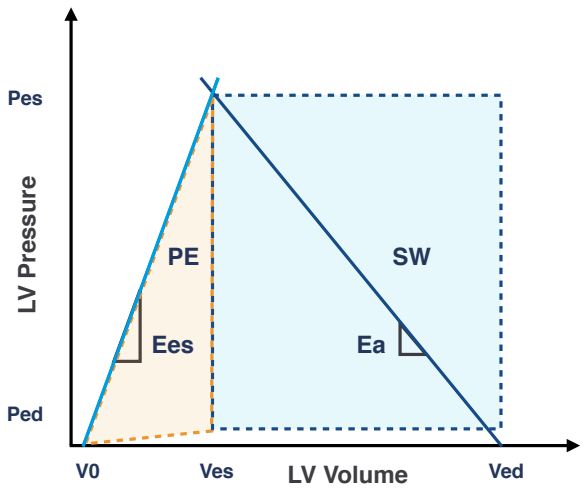

Figure 1: Left ventricular pressure-volume loop. Area inside is highlighted in blue. The slopes of LV elastance (E_{es}) and arterial elastance (E_a) are shown. V_{es}: end-systolic volume; P_{es}: end-systolic pressure; V_{ed}: end-diastolic volume; P_{es}: end-systolic pressure; V_0: volume-intercept; PE: potential energy.

2005]. Several methods have been proposed to derive the ESPVR from a single, steady-state beat [Chen et al., 2001; Kjørstad et al., 2002; Senzaki et al., 1996; Shishido et al., 2000; Takeuchi et al., 1991], with promising and reliable results. The single-beat method ultimately facilitates ESPVR estimation particularly when coupled with emerging noninvasive techniques to measure pressures and volumes in the clinical setting [Ten Brinke et al., 2010].

In this study, it is presented a computational software for researchers to manage physiological PV data that takes full advantage of single-beat method to estimate beat-to-beat LV and arterial physiologic properties. This software was used to capture instantaneous and dynamic hemodynamic changes in ventriculo-arterial coupling and cardiac performance in in-vivo rabbits during acute cardiovascular perturbations, including short term reflexes (mechano- and chemoreflexes) and diseases (myocardial infarction).

1. Background

1.1. Cardiovascular regulation

In this study, three mechanisms of autonomic balance of the cardiac system are analyzed: **(1)** cardiac baroreflex (BR), **(2)** arterial chemoreflex (CR) and **(3)** von Bezold-Jarisch reflex (BJR).

The cardiac baroreflex modulates a spontaneous fluctuation in the BP in an opposite fluctuation of HR by a negative feedback loop [Jordan et al., 2002]. When BP is elevated due to an afterload stimulation, baroreceptor afferents increase their firing rate, resulting in a decrease of impulses transmitted from autonomic nervous system to the heart and blood vessels, through the efferent sympathetic pathways. This causes the heart rate to slow down and peripheral blood vessels to dilate, thus decreasing BP back to normal [Spyer, 1989].

The arterial chemoreflex is a critical mechanism of control and regulation of the ventilatory responses [Wade et al., 1970], ensuring oxygen demand is met in various physiological conditions. Whenever arterial pressure of O_2 exceeds a critical level, arterial chemoreceptors become stimulated, resulting in a decrease of sympathetic nervous activity and, thus, depression of ventilation rate, mean arterial BP and HR to compensate the high levels of arterial pressure of O_2.

The von Bezold-Jarisch reflex, also known as cardiopulmonary reflex, is an inhibitory reflex induced by the stimulation of heart's receptors, either chemical or mechanical. When the heart's receptors sense stimuli, due to the presence of chemical hazards absorbed in the blood, cardiopulmonary afferent fibers are activated, causing a massive stimulation of parasympathetic and inhibition of the sympathetic activity. This results in a profound and simultaneous reduction in arterial BP and HR [Coleridge and Coleridge, 1980; Krayer, 1961].

1.2. Left ventricle end-systolic elastance as contractility index

In ventricular ejection, arterial pressure increases and the stroke volume (SV) is transferred into the aorta. The end-systolic volume (V_{es}) is a function of intrinsic cardiac contractility and arterial pressure: for the same V_{ed} and contractility, if arterial pressure at systole was less, then V_{es} would also be lower and SV greater, resulting in a PV loop shift to the left. Nothing else would be modified about the heart or arterial system properties [Gupta et al., 1989]. The resultant potential end-systolic PV points possible as arterial pressure is independently varied describe the end-systolic PV relationship (ESPVR). Its slope is the LV end-systolic elastance (E_{es}). E_{es} ($mmHg/mL$) provides a useful, load independent measurement of myocardial contractility and systolic function [Sagawa et al., 1977]. Since LV performance is not only influenced by ventricular stiffness, but also by biochemical and geometric properties [Borlaug and Kass, 2011], E_{es} should be considered as a measure which integrates LV systolic function, as well as the complex and modulating effects of the functional, structural and geometric characteristics of the LV and its contractile efficiency [Kass, 2002].

$$E_{es} = \frac{P_{es}}{V_{es} - V_0} \tag{1}$$

in which P_{es} represents LV end-systolic pressure ($mmHg$), V_{es} (mL) LV end-systolic volume and V_0 (mL) the intercept in the volume axis.

Several authors have proposed methods for computing the ESPVR from a single PV loop. [Takeuchi et al., 1991] simulated end-systolic isovolumic pressure by cosine fitting of the pressure curve, as done by [Sunagawa et al., 1980], to locate a theoretical maximum pressure P_{iso} that would be attained if ejection did not take place. The E_{es} is then computed as the slope of the line connecting the point defined by (V_{ed}, P_{max}) to the end-systolic point on the PV loop. Other authors relived on a time-varying elastance model to derive E_{es} [Chen et al., 2001; Senzaki et al., 1996; Shishido et al., 2000]. Recently, Ten Brinke et al. [2010] using Takeuchi et al.'s technique proposed a modified fitting scheme that would achieve good estimations of intercept volumes.

In this study, ESPVR were estimated following the single-beat method proposed by Ten Brinke et al. [2010]. Maximal pressure of an isovolumetric beat, P_{max}, is determined by fitting a fifth-order polynomial to the LV pressure curve, excluding all data points that lie after dP/dt_{max} and before dP/dt_{min} and those after the time-point when dP/dt increased above 15% of dP/dt_{min}.

1.3. Effective arterial elastance

The arterial system, as afterload, can also be assessed from the PV loop and can be characterized by its elastance. E_a ($mmHg/mL$) corresponds to the total load imposed on the LV, covering the complex association of different arterial properties, including total arterial compliance, characteristic impedance, peripheral arterial resistance (PVR) and diastolic time intervals [Sunagawa et al., 1983]. Mathematically, it is approximated by the ratio of P_{es} to stroke volume SV [Kelly et al., 1992].

1.4. Ventriculo-arterial coupling

A contractility or arterial tone that is too high or too low decouples the natural function of the cardiovascular system, leading to cardiac failure independent of myocardial ischemia and related systemic disease processes [Guarracino et al., 2013]. When LV ejects blood into the arterial system, LV workload and arterial system optimally match one another, which can be quantified by ventriculo-arterial (V-A) coupling analysis. This optimization is performed without excessive changes in LV pressure, and the mechanical energy of LV ejection is completely transferred from the ventricle to the peripheral vascular system [Kelly et al., 1992; Sunagawa et al., 1983]. V-A coupling can be defined as the ratio of elastances (E_a/E_{es}).

The V-A coupling ratio has been consistently demonstrated to be a reliable and effective measure of cardiovascular performance [Guarracino et al., 2007; Suga, 1969; Sunagawa et al., 1983]. De Tombe et al. [1993] and other investigators have demonstrated that the efficiency of the cardiovascular system is optimal when E_a/E_{es} is in the interval $0.3 - 1.3$. This range is also observed in dogs and cats, suggesting that it has been conserved through mammalian evolution [Chantler et al., 2008].

The role of V-A coupling in the assessment of cardiovascular function is becoming very clear, offering new and complementary perspectives for understanding how both heart and arterial systems work together, in order to optimize cardiovascular efficiency. E_a/E_{es} ratio has become considerably useful in characterizing pathophysiology of altered hemodynamic profiles and testing the effectiveness of treatments [Guarracino et al., 2013].

1.5. Cardiac workload and total energy consumption

The area inside the left ventricle PV loop during a single cardiac cycle represents the workload (SW) produced by the ventricle to eject blood. SW ($mmHg \cdot mL$, unit of energy) is maximal when all the energy from the ventricles is transferred to the arterial system, which occurs when $E_a = E_{es}$ [Burkhoff and Sagawa, 1986; Glower et al., 1985]. The ratio of SW to SW_{max} quantifies the degree of optimality of the afterload (Q_{load}).

The pressure-volume area (PVA) ($mmHg \cdot mL$) is equal to the sum of LV potential energy (PE) and SW, representing all the energy that the ventricle requires to contract and pump blood under the given loading conditions [Suga, 2003]. PVA corresponds to the total mechanical energy of a ventricular beat and has a linear correlation with myocardial oxygen consumption [Hayashi et al., 2000; Suga et al., 1983]. PE is the mechanical energy available in the ventricle at end-systole, which is not converted into external work and dissipates as heat during relaxation.

The ratio of SW to PVA corresponds to the efficiency of cardiac contraction (CWE), also known as efficiency of the heart. CWE is a function of ventricular loading and inotropic state, increasing with contractility enhancement and decreasing with afterload [Nozawa et al., 1988].

2. Methods and implementation

2.1. In-vivo measurements

The data was acquired from controlled experiments in fourteen anesthetized, paralyzed and artificially ventilated New Zealand rabbits (3.35 ± 0.85 kg) of either sex. The protocol was conformed according to national laws and international guidelines.

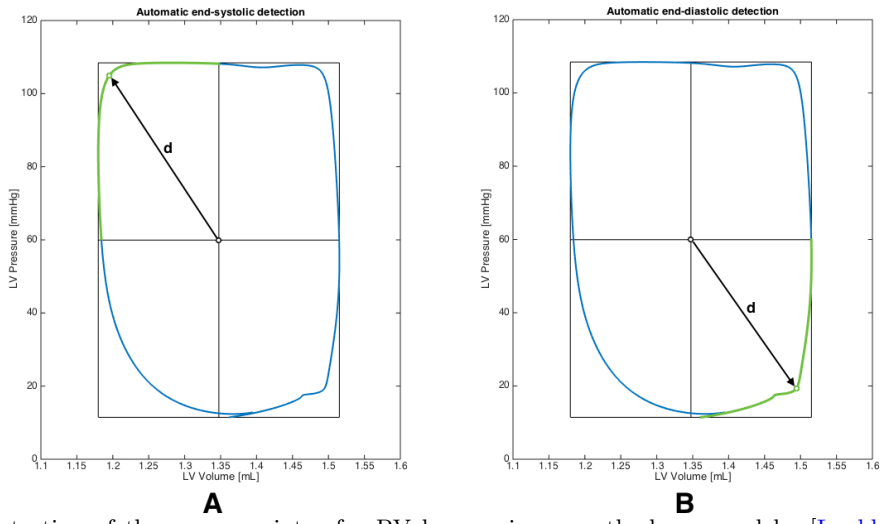

Figure 2: Detection of the corner points of a PV loop, using a method proposed by [Lankhaar et al., 2009]. For each quadrant, corner points are defined as the point where the distance to the center of the circumscribing rectangle is maximal.

An intraventricular impedance catheter was used to measure simultaneously LV pressure and volume. All recorded signals were digitized at a sampling rate of 100 Hz.

Arterial chemoreflex was evoked by injection of lobeline (20 $\mu g/kg$, $pH = 7.4 \pm 0.1$) into the carotid sinus, whereas the Bezold-Jarisch reflex was evoked by cardiac injection of ATP (0.1 mL; 20 mM, $pH = 5.4 \pm 0.1$). Cardiac baroreflex was assessed by inflating a Swan-Ganz balloon in the descending aorta, to raise peripheral resistance. Before repetition of the test, 30 minutes were allowed to elapse. Heart ischemia was provoked by ligation of the descending coronary artery.

Detailed information on the experimental protocol is presented in Rocha et al. [2003a] and Rosario et al. [2003].

2.2. Graphical user interface

In this work, a custom Graphical User Interface was designed and implemented in Matlab to provide a easy-to-use framework for researchers to manage stored pressure-volume data and to compute single-beat cardiovascular parameters, using the algorithms and methods described throughout this subsection.

PV data preparation. The first stage is data selection and filtering. The GUI provides two ways of removing random and unpredictable noise from pressure-volume data. A band-pass filter is used to enhance edges, by suppressing low frequencies, while reducing the noise at the same time, by attenuating high frequencies. A Savitzky-Golay filter is a particular type of low-pass filter well-adapted for data smoothing that replace each data point by a local average of surrounding data points, making it suitable for noise reduction without too much bias.

Systole identification. In the second stage, each cardiac cycle's end-diastolic and end-systolic points are detected using an automatic algorithm proposed in Lankhaar et al. [2009]. For each cardiac cycle, the distance $d(t_i)$ of each point in the PV loop's corners to its center (V_c, P_c) is calculated, and the point with the maximal distance is defined as the corner point (see **Figure 2**). The bottom-right and left-upper corners correspond to the end-diastolic and end-systolic points, respectively.

$$d(t_i) = \sqrt{\left[\frac{V(t_i) - V_c}{\Delta V}\right]^2 + \left[\frac{P(t_i) - P_c}{\Delta P}\right]^2} \quad (2)$$

where $\Delta V = V_{max} - V_{min}$, $\Delta P = P_{max} - P_{min}$, $V_c = (V_{max} + V_{min})/2$ and $P_c = (P_{max} + P_{min})/2$. For end-systolic point detection, the interval for t_i only considers points with volume smaller than V_c and pressure larger than P_c; for end-diastolic point detection, the interval considers points with volume larger than V_c and pressure smaller than P_c.

Every systole must be confirmed by the user, to reduce any possible misestimation that might influence the final results. If the user notices the systole was poorly identified, a correction can be added using a complementary manual process.

End-systolic elastance estimation. In this stage, E_{es} is estimated using a single-beat method proposed in Ten Brinke et al. [2010] (see **Figure 3**). Afterwards, LV cardiovascular properties are automatically derived from E_{es}, computing indexes that characterize V-A coupling, LV systolic performance and cardiac efficiency.

Visualization tool. In the last stage, results can be interactively plotted, compared and saved. The aim of the visualization tool is to present data

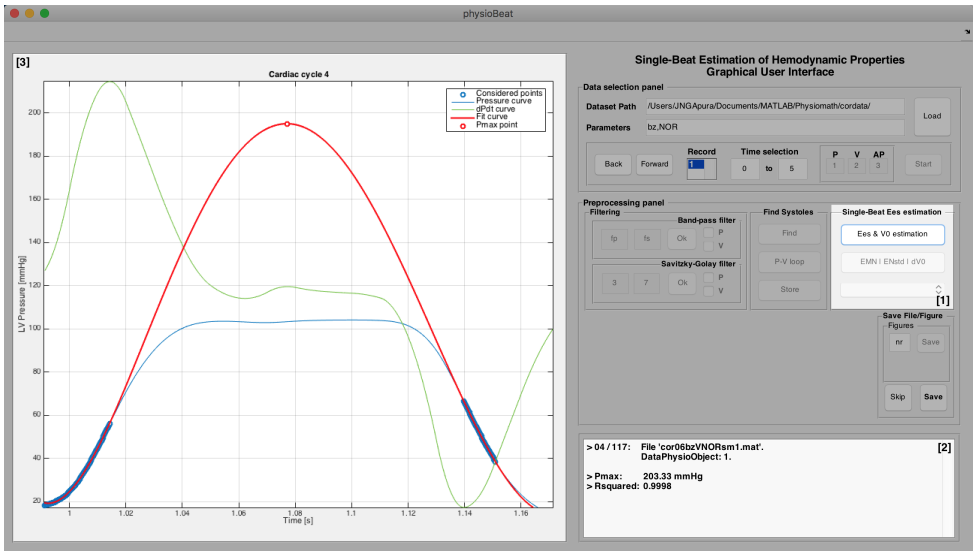

Figure 3: Representation of Ten Brinke et al.'s single-beat method used to estimate the isovolumic pressure curve and its maximum, P_{max}, from a single ejecting beat. The isovolumetric pressure curve (in red) is fitted through the isovolumic contraction and relaxation periods. The pressure curve is represented in blue and dP/dt is represented in green.

in such a way that even someone without any background in PV data analysis is able to digest the results, and easily uncover specific trends or make data-driven conclusions.

2.3. Statistical analysis

Longitudinal results were organized in three different measurements: at baseline conditions (`M1`), immediately after reflex stimulation (`M2`) and at the reflex *plateau* (`M3`). The last measurement is determined by visual inspection of changes in arterial pressure and LV pressure and volume. In order to reduce the effect of the artificial respiration, 20 consecutive cardiac beats are selected for each measurement.

In order to visually analyze trends and patterns over time, results are expressed as beat-to-beat mean ± standard deviation. Linear mixed-effects models for repeated measurements was employed to discover patterns of systematic variation across groups of rabbits (within-subject variation), as well as aspects of random variation that can distinguish between individual rabbits (between-subject variation). Moreover, differences of means between groups were estimated to examine the effect of myocardial infarction on the cardiovascular properties in study and how this might compromise the heart's response to each reflex stimulation. Statistical tests were performed in SPSS Statistics 12.0.

3. Results and discussion

In this section, all the results obtained are taken into consideration, being only displayed the relevant ones. Ventriculo-arterial coupling and cardiac performance are analyzed for each cardiovascular reflex, evoked under normal conditions, in order to capture and further understand how heart's mechanical properties change during these short-term reflexes. This is followed by a thorough description of the major hemodynamic changes in a pathological cardiovascular system. Finally, in order to capture how acute interventions might compromise the heart's response during reflex activation, cardiovascular coupling, performance and efficiency are addressed for each reflex, once more.

3.1. Autonomic reflexes in an intact cardiovascular system

The closed-loop network of cardiovascular reflexes in study, in normal conditions, revealed a balanced control of induced homeostatic perturbations by modeling both cardiac contractility and arterial input impedance, with consequent changes in stroke work, in such a way that ventriculo-arterial coupling, mechanical ratio and cardiac energetic efficiency were maintained between optimal values.

The cardiac baroreflex enhanced cardiac contractility and arterial tone to improve LV workload, obtained at a higher oxygen cost (**Figures 4 & 5 - left**). Since Q_{load} remained close to unity during reflex stimulation, this shows that the arterial system was able to extract maximal energy from the left ventricle [Burkhoff and Sagawa, 1986; Glower et al., 1985]. Comparing Q_{load} and CWE indexes, it seems the energy transmission was more optimized than was oxygen consumption.

Lobeline-induced arterial chemoreflex revealted a statistically significant increase in both contractility and arterial input impedance, with simultaneous

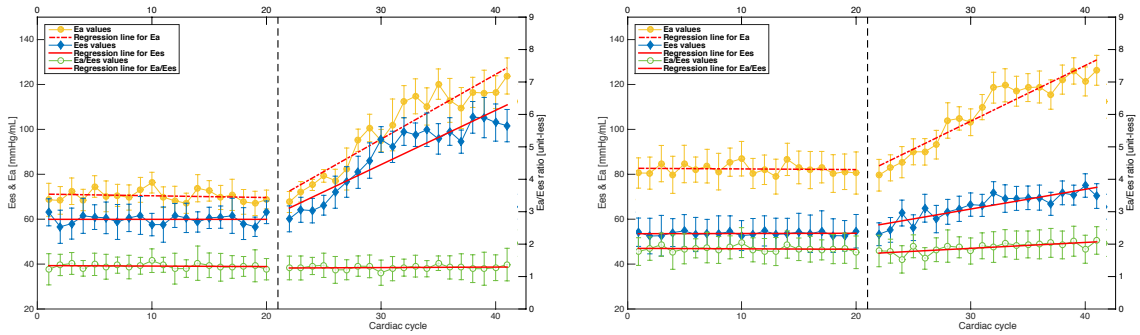

Figure 4: Beat-to-beat mean E_{es}, E_a and E_a/E_{es}, evoked on the stimulation of the baroreceptors under normal conditions (**left**, $n = 42$) and after acute myocardial infarction (**right**, $n = 27$), for measurements `M1-2`. Bars denote standard deviation.

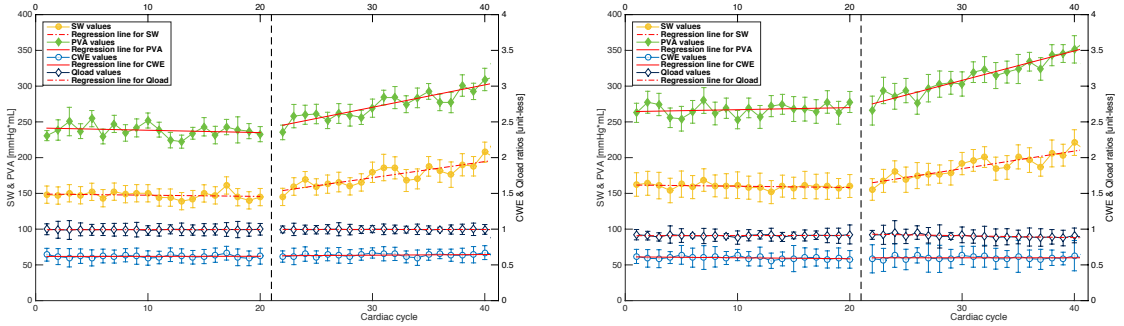

Figure 5: Beat-to-beat mean SW, PVA, Q_{load} and CWE, evoked on the stimulation of the baroreceptors under normal conditions (**left**, $n = 42$) and after acute myocardial infarction (**right**, $n = 27$), for measurements `M1-2`. Bars denote standard deviation.

	Measurement M1				Measurement M2				
	μ	σ	a	b	μ	σ	a	b	$p-value$
E_a	70.394	2.605	-0.079	71.220	99.979	18.146	2.888	8.992	<0.001*
E_{es}	59.936	2.010	0.000	59.936	87.944	15.403	2.418	11.778	<0.001*
E_a/E_{es}	1.176	0.061	-0.001	1.190	1.137	0.078	0.001	1.093	0.14
SW	147.380	4.967	-0.169	149.150	175.342	15.465	2.251	104.436	<0.001*
PVA	238.127	8.639	-0.327	241.557	275.121	20.267	3.132	176.462	<0.001*
Q_{load}	0.993	0.004	0.000	0.993	0.994	0.003	-0.000	0.995	0.46
CWE	0.619	0.018	0.000	0.618	0.627	0.020	0.001	0.597	0.42

	Measurement M1				Measurement M2				
	μ	σ	a	b	μ	σ	a	b	$p-value$
E_a	67.178	2.490	-0.032	67.516	94.077	16.605	2.675	9.829	<0.001*
E_{es}	36.221	0.854	0.011	36.106	49.367	6.359	0.946	19.560	<0.001*
E_a/E_{es}	1.856	0.079	-0.001	1.871	1.898	0.154	0.018	1.324	0.19
SW	159.944	3.546	-0.179	161.823	188.270	16.291	2.461	110.738	<0.001*
PVA	267.218	8.326	0.286	264.212	314.260	25.478	4.117	184.560	<0.001*
Q_{load}	0.910	0.012	0.000	0.908	0.904	0.022	-0.003	0.987	0.26
CWE	0.599	0.020	-0.001	0.613	0.598	0.022	0.000	0.599	0.22

Table 1: Mean (μ), standard deviation (σ) and fit coefficients (a, b and R^2) of E_{es}, E_a, E_a/E_{es}, SW, PVA, Q_{load} and CWE in baroreflex *stimulation* under normal conditions (**left**, $n = 42$) and after acute myocardial infarction (**right**, $n = 27$), discriminated by measurement.

reduction of workload and oxygen intake (**Figures 6 & 7 - left**). Q_{load} remained close to unity throughout the lobeline-induced reflex, which indicates that the arterial system was able to extract maximal energy from the left ventricle. However, a decrease in SW also implicated a loss in energy transmitted to the arterial system, thus influencing total peripheral resistance. Comparing Q_{load} and CWE indexes, oxygen consumption was not optimized.

The cardiopulmonary reflex is provoked a simultaneous reduction in cardiac contractility, workload and oxygen demand (**Figures 8 & 9 - left**), as a way to protect the heart from injected ATP. Q_{load} remained close to unity. Although CWE was not optimized, results indicate that the cardiovascular system might have attempted to increase cardiac work efficiency during the ATP-induced von Bezold-Jarisch reflex.

3.2. Effect of acute myocardial infarction on heart's mechanical properties

Coronary ligation contributed to considerable changes in heart's mechanical properties. Results showed an impairment in myocardial contractility throughout all cardiovascular reflexes in analysis (compare **left** and **right figures 4-9**), as a consequence of myocyte hyperthophy and alterations in LV architecture due to an oddly distributed wall tension [Jegger et al., 2007]. Arterial input impedance was not affected. Since results reported

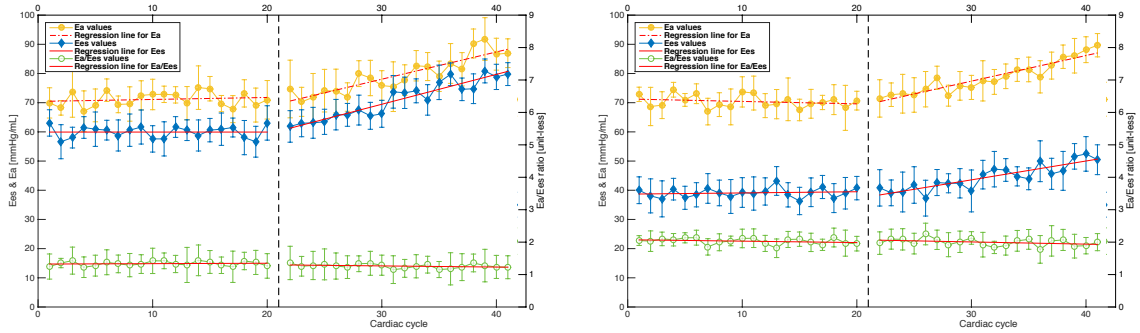

Figure 6: Beat-to-beat mean E_{es}, E_a and E_a/E_{es}, evoked on the stimulation of the arterial chemoreceptors under normal conditions (**left**, $n = 26$) and after acute myocardial infarction (**right**, $n = 11$), for measurements `M1-2`. Bars denote standard deviation.

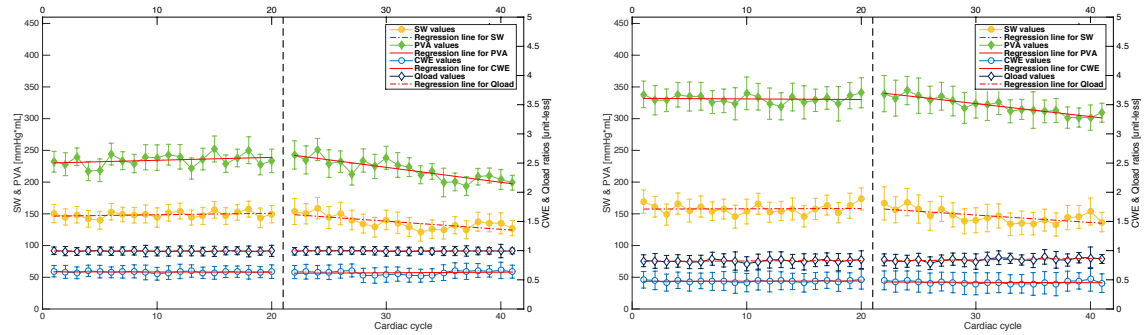

Figure 7: Beat-to-beat mean SW, PVA, Q_{load} and CWE, evoked on the stimulation of the arterial chemoreceptors under normal conditions (**left**, $n = 26$) and after acute myocardial infarction (**right**, $n = 11$), for measurements `M1-2`. Bars denote standard deviation.

	Measurement M1				Measurement M2				
	μ	σ	a	b	μ	σ	a	b	$p-value$
E_a	71.143	3.085	0.085	70.251	79.450	6.195	0.934	50.036	<0.001*
E_{es}	59.736	1.990	0.000	59.736	71.000	6.423	1.024	38.735	<0.001*
E_a/E_{es}	1.188	0.062	0.001	1.142	1.132	0.097	-0.002	1.220	0.23
SW	148.621	4.717	0.233	146.172	136.506	10.595	-1.276	176.700	<0.001*
PVA	234.629	9.483	0.460	229.798	219.733	16.439	-2.358	294.024	<0.001*
Q_{load}	0.992	0.005	-0.000	0.993	0.994	0.004	-0.000	0.994	0.20
CWE	0.634	0.012	-0.000	0.636	0.622	0.033	0.001	0.590	0.34

	Measurement M1				Measurement M2				
	μ	σ	a	b	μ	σ	a	b	$p-value$
E_a	70.393	2.147	-0.083	71.269	78.700	5.532	0.877	51.062	<0.001*
E_{es}	39.099	1.620	0.041	38.670	44.527	4.364	0.646	24.170	<0.001*
E_a/E_{es}	1.803	0.085	-0.004	1.844	1.774	0.101	-0.006	1.964	0.33
SW	157.940	7.516	0.042	157.495	146.349	10.611	-1.175	183.355	<0.001*
PVA	331.037	6.199	-0.093	332.013	320.598	12.995	-2.048	385.098	<0.001*
Q_{load}	0.824	0.021	0.001	0.816	0.831	0.037	0.003	0.766	0.37
CWE	0.477	0.017	0.000	0.474	0.471	0.034	-0.001	0.477	0.44

Table 2: Mean (μ), standard deviation (σ) and fit coefficients (a, b and R^2) of E_{es}, E_a, E_a/E_{es}, SW, PVA, Q_{load} and CWE in arterial chemoreflex *stimulation* under normal conditions (**left**, $n = 26$) and after acute myocardial infarction (**right**, $n = 11$), discriminated by measurement.

E_a almost twice as large as E_{es}, there is evidence of an uncoupled cooperation between ventricle and arterial systems, with the V-A ratio spanning far from the optimal conditions. These results suggest that arterial tone is maintained within the physiological range at the expense of the deterioration of the energy transfer from the left ventricle to the arterial system [Asanoi et al., 1995].

In order to maintain adequate perfusion of vital organs, the failing heart must generate sufficient blood pressure and flow to overcome the peripheral resistance. The infarted heart's response is to dilate its left ventricle, in order to maintain an adequate blood pressure and, thus, compensate for the depressed contractility. The pathological ventricular enlargement, as confirmed by the increased values in V_{ed} and V_{es} in ischemic hearts, seemed to be a consequence of compensation and not a limiting factor to depressed hemodynamics and energetics. Also, it is interesting to point out that this heart's dilation was achieved without a significant change in SV, when compared to the control group, which clearly confirms SV as a poor indicator of heart failure or cardiac dysfunction [Maeder and Kaye, 2009].

Results also showed a depression in both Q_{load} and CWE values. Since the heart is no longer able to contract at its full potential due to my-

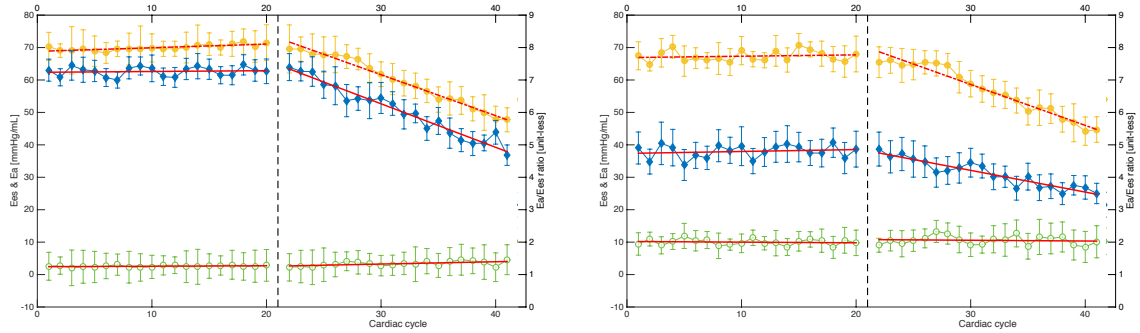

Figure 8: Beat-to-beat mean E_{es}, E_a and E_a/E_{es}, evoked on the stimulation of the cardiopulmonary receptors under normal conditions (**left**, $n = 23$) and after acute myocardial infarction (**right**, $n = 13$), for measurements `M1-2`. Bars denote standard deviation.

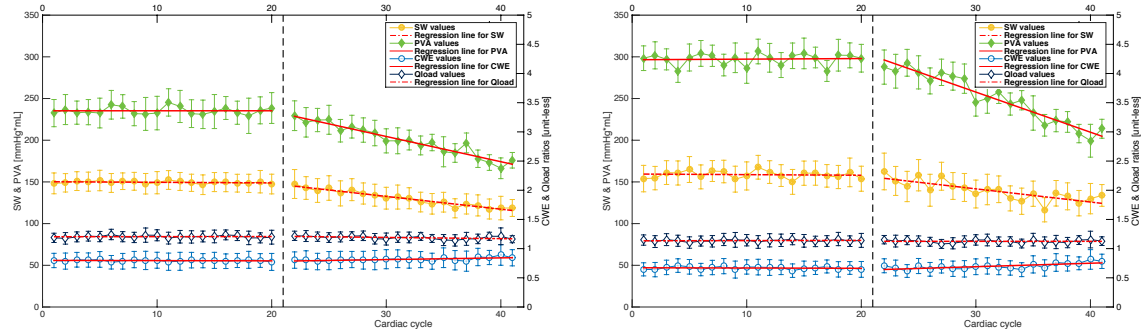

Figure 9: Beat-to-beat mean SW, PVA, Q_{load} and CWE, evoked on the stimulation of the cardiopulmonary receptors under normal conditions (**left**, $n = 23$) and after acute myocardial infarction (**right**, $n = 13$), for measurements `M1-2`. Bars denote standard deviation.

	Measurement M1				Measurement M2				
	μ	σ	a	b	μ	σ	a	b	$p-value$
E_a	69.998	1.901	0.113	68.816	59.726	7.542	-1.262	99.476	<0.001*
E_{es}	62.630	1.436	0.025	62.364	50.650	8.131	-1.342	92.920	<0.001*
E_a/E_{es}	1.118	0.025	0.001	1.104	1.137	0.089	0.006	0.976	0.26
SW	149.492	1.476	-0.072	150.247	130.325	9.349	-1.533	178.621	<0.001*
PVA	235.308	4.356	0.000	235.308	199.943	18.541	-3.025	295.236	<0.001*
Q_{load}	0.964	0.015	0.000	0.963	0.956	0.020	-0.002	1.003	0.15
CWE	0.635	0.011	-0.000	0.639	0.643	0.022	0.002	0.569	0.17

	Measurement M1				Measurement M2				
	μ	σ	a	b	μ	σ	a	b	$p-value$
E_a	67.348	1.695	0.042	66.910	56.726	7.637	-1.262	96.476	<0.001*
E_{es}	37.980	2.021	0.059	37.359	31.128	4.226	-0.670	52.219	<0.001*
E_a/E_{es}	1.777	0.083	-0.002	1.796	1.826	0.123	-0.002	1.891	0.14
SW	158.694	4.424	-0.074	159.469	158.694	4.424	-0.074	159.469	<0.001*
PVA	297.260	6.911	0.071	296.510	250.505	29.574	-4.813	402.108	<0.001*
Q_{load}	0.910	0.013	0.000	0.907	0.905	0.021	-0.000	0.900	0.59
CWE	0.534	0.019	-0.000	0.538	0.559	0.041	0.005	0.410	0.11

Table 3: Mean (μ), standard deviation (σ) and fit coefficients (a, b and R^2) of E_{es}, E_a, E_a/E_{es}, SW, PVA, Q_{load} and CWE in von Bezold-Jarisch reflex *stimulation* under normal conditions (**left**, $n = 23$) and after acute myocardial infarction (**right**, $n = 13$), discriminated by measurement.

ocardial necrosis, cardiac work increased as an effort to maintain the arterial tone within the physiological range. Interestingly, impairment in myocardial contractility did not necessarily result in a deterioration of cardiac work performance between groups. A possible explanation for the improved left ventricle performance lies on increased wall tension. Increased end-systolic pressure could act on mechanical stretch-activated channels, creating a transmembrane pressure gradient that could be sufficient to increase calcium release [Morris, 1990].

Moreover, the overall augmentation of LV stroke work was obtained at a higher oxygen cost. Stahl et al. [1988] also found a significant increase in mean oxygen consumption in dog hearts with impairment of contractile function. Unbalanced increase in SW and PVA indexes resulted in an overall decrease in cardiac work efficiency, as it would be expected from a failing heart.

3.3. Autonomic reflexes in a pathological system

Activation of cardiovascular reflexes in ischemic hearts revealed similar hemodynamic responses as in the control group, despite an evident impairment of cardiovascular system. For all reflexes, induced homeostatic perturbations were controlled through modeling LV contractility, arterial input impedance and LV stroke work.

The cardiac baroreflex targeted an increase in cardiac contractility and arterial tone to improve cardiac stroke work (**Figures 4 & 5 - right**). Surprisingly, acute myocardial infarction did not seem to compromise how SW is affected by the reflex. Total energy expenditure was compromised, suggesting an abnormal oxygen intake by the ischemic heart. Results show an attenuation of CWE change in ischemic hearts.

The arterial chemoreflex in ischemic hearts elicited an increase in contractility and arterial input impedance, with simultaneous fall in both cardiac stroke work and oxygen demand (**Figures 6 & 7 - right**). Interestingly, results suggest the infarcted heart chose to optimize energy transmission to the arterial system over cardiac efficiency.

Finally, activation of ATP-induced von Bezold-Jarisch reflex resulted in a significant decrease in LV contractility, stroke work and heart's energy consumption (**Figures 8 & 9 - right**), protecting the heart from hazardous chemicals. Comparing Q_{load} and CWE indexes, this cardioprotective reflex chooses to optimize energetic efficiency, rather than energy transmission to the arterial system.

4. Conclusions

The closed-loop network of cardiovascular reflexes in study revealed a balanced control of induced homeostatic perturbations by modeling both cardiac contractility and arterial input impedance, with consequent changes in stroke work, in such a way that ventriculo-arterial coupling, mechanical ratio and cardiac energetic efficiency were maintained between optimal values. While the cardiac baroreflex enhanced cardiac contracility and arterial tone to improve stroke work, the arterial chemoreflex focused on reducing oxygen intake. The cardiopulmonary reflex provoked a reduction in both cardiac workload and oxygen demand, as a way to protect the heart from injected ATP. Each reflex optimized the cardiac work and energetic efficiencies dissimilarly.

Acute myocardial infarction contributed to considerable changes in heart's mechanical properties. Cardiac contractility was significantly reduced. Arterial input impedance was not altered, providing evidence that the arterial tone was maintained within the physiological range at the expense of the deterioration of the energy flow between left ventricle and arterial system. As a result, ventriculo-arterial coupling became compromised. End-diastolic and end-systolic volumes were augmented, as a consequence of left ventricular enlargement to compensate for the depressed contractility, though stroke volume was unaffected. Interestingly, the workload was enhanced as an effort to maintain the arterial tone within the optimal physiological range, with no evidence of deterioration. Since the overall improvement of stroke work was obtained at a higher oxygen cost, cardiac work efficiency and ratio of stroke work to its theoretical maximum were depressed.

Activation of cardiovascular reflexes in ischemic hearts revealed similar hemodynamic responses as in the control group, despite an evident impairment of cardiovascular system. For all reflexes, induced homeostatic perturbations were controlled through modeling LV contractility, arterial input impedance and LV stroke work. The cardiac baroreflex focused in improving the left ventricle stroke work, whereas the lobeline-induced arterial chemoreflex targeted a reduction in the heart's abnormal oxygen intake. The von Bezold-Jarisch reflex reduced heart's workload and energetic demand by choosing to optimize cardiac energetic efficiency, rather than energy transmission to the arterial system.

The proposed methodology disclosed considerable results regarding the autonomic balance of the cardiac system in the point of view of cardiovascular efficiency and ventriculo-arterial coupling during acute cardiovascular perturbations, including short term reflexes (mechano- and chemoreflexes) and diseases (myocardial infarction). The major advantage of the developed computational software is, undoubtedly, the ability to aggregate PV data in a clear and physiologically relevant picture, and to accurately compute a wide variety of single-beat indexes that can characterize and quantify chamber contractility and performance.

Given its advantages, future studies should focus on characterizing performance and ventriculo-arterial coupling in different clinical settings, such as drug testing and device therapy. Recent literature show that activation of cardiovascular chemoreceptors after myocardial infarction was partially reversed by losartan microinjection at the level of the central nervous system, suggesting that its angiotensin receptors were involved in the control of the autonomic outflow of cardiovascular reflexes [Rocha et al., 2003b; Rosario et al., 2003]. This analysis will certainly allow to better understand autonomic modulation of cardiovascular reflexes.

Acknowledgements

I would like to thank my supervisors Professor Adélia Sequeira and Professor Dr. Luís Brás Rosário for all the help and motivation given throughout the entire development of this work.

This study was supported by project grant "PHYSIOMATH - Mathematical and Computational Modelling of Human Physiology", FCT Project EXCL/MAT-NAN/0114/2012.

References

[1]: **Asanoi, H., Kameyama, T. and Ishizaka, S.** [1995], Ventriculo-arterial load matching of failing hearts, *in* 'Cardiac Energetics: From Emax to Pressure-Volume Area', Springer, pp. 157–169.

[2]: **Borlaug, B. A. and Kass, D. A.** [2011], 'Ventricular–vascular interaction in heart failure', *Cardiology clinics* **29**(3), 447–459.

[3]: **Burkhoff, D., Mirsky, I. and Suga, H.** [2005], 'Assessment of systolic and diastolic ventricular properties via pressure-volume analysis: a guide for clinical, translational, and basic researchers', *American Journal of Physiology-Heart and Circulatory Physiology* **289**(2), H501–H512.

[4]: **Burkhoff, D. and Sagawa, K.** [1986], 'Ventricular efficiency predicted by an analytical model', *American Journal of Physiology-Regulatory, Integrative and Comparative Physiology* **250**(6), R1021–R1027.

[5]: **Chantler, P. D., Lakatta, E. G. and Najjar, S. S.** [2008], 'Arterial-ventricular coupling: mechanistic insights into cardiovascular performance at rest and during exercise', *Journal of applied physiology* **105**(4), 1342–1351.

[6]: **Chen, C.-H., Fetics, B., Nevo, E., Rochitte, C. E., Chiou, K.-R., Ding, P.-A., Kawaguchi, M. and Kass, D. A.** [2001], 'Noninvasive single-beat determination of left ventricular end-systolic elastance in humans', *Journal of the American College of Cardiology* **38**(7), 2028–2034.

[7]: **Coleridge, H. M. and Coleridge, J. C. G.** [1980], 'Cardiovascular afferents involved in regulation of peripheral vessels', *Annual Review of Physiology* **42**(1), 413–427.

[8]: **De Tombe, P. P., Jones, S., Burkhoff, D., Hunter, W. C. and Kass, D. A.** [1993], 'Ventricular stroke work and efficiency both remain nearly optimal despite altered vascular loading', *American Journal of Physiology-Heart and Circulatory Physiology* **264**(6), H1817–H1824.

[9]: **Glower, D. D., Spratt, J. A., Snow, N. D., Kabas, J., Davis, J., Olsen, C., Tyson, G., Sabiston, D. and Rankin, J.** [1985], 'Linearity of the frank-starling relationship in the intact heart: the concept of preload recruitable stroke work.', *Circulation* **71**(5), 994–1009.

[10]: **Guarracino, F., Baldassarri, R. and Pinsky, M. R.** [2013], 'Ventriculo-arterial decoupling in acutely altered hemodynamic states', *Crit Care* **17**(2), 213.

[11]: **Guarracino, F., Cariello, C., Danella, A., Doroni, L., Lapolla, F., Stefani, M., Baldassarri, R. and Vullo, C.** [2007], 'Effect of levosimendan on ventriculo-arterial coupling in patients with ischemic cardiomyopathy', *Acta anaesthesiologica Scandinavica* **51**(9), 1217–1224.

[12]: **Gupta, K. B., Bavaria, J., Ratcliffe, M., Edmunds, L. and Bogen, D.** [1989], 'Measurement of end-systolic pressure-volume relations by intra-aortic balloon occlusion.', *Circulation* **80**(4), 1016–1028.

[13]: **Hayashi, K., Shigemi, K., Shishido, T., Sugimachi, M. and Sunagawa, K.** [2000], 'Single-beat estimation of ventricular end-systolic elastance–effective arterial elastance as an index of ventricular mechanoenergetic performance', *The Journal of the American Society of Anesthesiologists* **92**(6), 1769–1776.

[14]: **Jegger, D., Mallik, A. S., Nasratullah, M., Jeanrenaud, X., Da Silva, R., Tevaearai, H., Von Segesser, L. K. and Stergiopulos, N.** [2007], 'The effect of a myocardial infarction on the normalized time-varying elastance curve', *Journal of Applied Physiology* **102**(3), 1123–1129.

[15]: **Jordan, J., Tank, J., Shannon, J. R., Diedrich, A., Lipp, A., Schröder, C., Arnold, G., Sharma, A. M., Biaggioni, I., Robertson, D. et al.** [2002], 'Baroreflex buffering and susceptibility to vasoactive drugs', *Circulation* **105**(12), 1459–1464.

[16]: **Kass, D. A.** [2002], 'Age-related changes in venticular–arterial coupling: pathophysiologic implications', *Heart failure reviews* **7**(1), 51–62.

[17]: **Kelly, R. P., Ting, C.-T., Yang, T.-M., Liu, C.-P., Maughan, W. L., Chang, M.-S. and Kass, D. A.** [1992], 'Effective arterial elastance as index of arterial vascular load in humans.', *Circulation* **86**(2), 513–521.

[18]: **Kjørstad, K. E., Korvald, C. and Myrmel, T.** [2002], 'Pressure-volume-based single-beat estimations cannot predict left ventricular contractility in vivo', *American Journal of Physiology-Heart and Circulatory Physiology* **282**(5), H1739–H1750.

[19]: **Krayer, O.** [1961], 'The history of the bezold-jarisch effect', *Naunyn-Schmiedebergs Archiv für experimentelle Pathologie und Pharmakologie* **240**(5), 361–368.

[20]: **Lankhaar, J.-W., Rövekamp, F. A., Steendijk, P., Faes, T. J., Westerhof, B. E., Kind, T., Vonk-Noordegraaf, A. and Westerhof, N.** [2009], 'Modeling the instantaneous pressure–volume relation of the left ventricle: a comparison of six models', *Annals of biomedical engineering* **37**(9), 1710–1726.

[21]: **Maeder, M. T. and Kaye, D. M.** [2009], 'Heart failure with normal left ventricular ejection fraction', *Journal of the American College of Cardiology* **53**(11), 905–918.

[22]: **Morris, C. E.** [1990], 'Mechanosensitive ion channels', *Journal of Membrane Biology* **113**(2), 93–107.

[23]: **Nozawa, T., Yasumura, Y., Futaki, S., Tanaka, N., Uenishi, M. and Suga, H.** [1988], 'Efficiency of energy transfer from pressure-volume area to external mechanical work increases with contractile state and decreases with afterload in the left ventricle of the anesthetized closed-chest dog.', *Circulation* **77**(5), 1116–1124.

[24]: **Rocha, I., Brás-Rosário, L., Amparo-Barros, M. and Silva-Carvalho, L.** [2003b], 'Angiotensin at1 receptor antagonist losartan and the defence reaction in the anaesthetised rat. effect on the carotid chemoreflex', *Experimental physiology* **88**(03), 309–314.

[25]: **Rocha, I., Rosário, L., De Oliveira, E., Barros, M. and Silva-Carvallho, L.** [2003a], 'Enhancement of carotid chemoreceptor reflex and cardiac chemosensitive reflex in the acute phase of myocardial infarction of the anesthetized rabbit', *Basic research in cardiology* **98**(3), 175–180.

[26]: **Rodriguez, D. A.-A., Durand, E., De Rochefort, L., Boudjemline, Y. and Mousseaux, E.** [2015], 'Simultaneous pressure–volume measurements using optical sensors and mri for left ventricle function assessment during animal experiment', *Medical engineering & physics* **37**(1), 100–108.

[27]: **Rosario, L., Rocha, I. and Silva-Carvalho, L.** [2003], Effect of losartan microinjections into the nts on the cardiovascular components of chemically evoked reflexes in a rabbit model of acute heart ischemia, *in* 'Chemoreception', Springer, pp. 423–431.

[28]: **Sagawa, K., Suga, H., Shoukas, A. A. and Bakalar, K. M.** [1977], 'End-systolic pressure/volume ratio: a new index of ventricular contractility', *The American journal of cardiology* **40**(5), 748–753.

[29]: **Senzaki, H., Chen, C.-H. and Kass, D. A.** [1996], 'Single-beat estimation of end-systolic pressure-volume relation in humans a new method with the potential for noninvasive application', *Circulation* **94**(10), 2497–2506.

[30]: **Shishido, T., Hayashi, K., Shigemi, K., Sato, T., Sugimachi, M. and Sunagawa, K.** [2000], 'Single-beat estimation of end-systolic elastance using bilinearly approximated time-varying elastance curve', *Circulation* **102**(16), 1983–1989.

[31]: **Spyer, K.** [1989], 'Neural mechanisms involved in cardiovascular control during affective behaviour', *Trends in neurosciences* **12**(12), 506–513.

[**32**]: **Stahl, L. D., Weiss, H. R. and Becker, L. C.** [1988], 'Myocardial oxygen consumption, oxygen supply/demand heterogeneity, and microvascular patency in regionally stunned myocardium.', *Circulation* **77**(4), 865–872.

[**33**]: **Suga, H.** [1969], 'Time course of left ventricular pressure-volume relationship under various end-diastolic volumes', *Japanese heart journal* **10**(6), 509–515.

[**34**]: **Suga, H.** [2003], 'Global cardiac function: mechano-energetico-informatics', *Journal of biomechanics* **36**(5), 713–720.

[**35**]: **Suga, H., Hisano, R., Hirata, S., Hayashi, T., Yamada, O. and Ninomiya, I.** [1983], 'Heart rate-independent energetics and systolic pressure-volume area in dog heart', *American Journal of Physiology-Heart and Circulatory Physiology* **244**(2), H206–H214.

[**36**]: **Sunagawa, K., Maughan, W. L., Burkhoff, D. and Sagawa, K.** [1983], 'Left ventricular interaction with arterial load studied in isolated canine ventricle', *American Journal of Physiology-Heart and Circulatory Physiology* **245**(5), H773–H780.

[**37**]: **Sunagawa, K., Yamada, A., Senda, Y., Kikuchi, Y., Nakamura, M., Shibahara, T. and Nose, Y.** [1980], 'Estimation of the hydromotive source pressure from ejecting beats of the left ventricle', *Biomedical Engineering, IEEE Transactions on* (6), 299–305.

[**38**]: **Takeuchi, M., Igarashi, Y., Tomimoto, S., Odake, M., Hayashi, T., Tsukamoto, T., Hata, K., Takaoka, H. and Fukuzaki, H.** [1991], 'Single-beat estimation of the slope of the end-systolic pressure-volume relation in the human left ventricle.', *Circulation* **83**(1), 202–212.

[**39**]: **Ten Brinke, E., Klautz, R., Verwey, H., Van Der Wall, E., Dion, R. and Steendijk, P.** [2010], 'Single-beat estimation of the left ventricular end-systolic pressure–volume relationship in patients with heart failure', *Acta physiologica* **198**(1), 37–46.

[**40**]: **Wade, J. G., Larson Jr, C. P., Hickey, R. F., Ehrenfeld, W. K. and Severinghaus, J. W.** [1970], 'Effect of carotid endarterectomy on carotid chemoreceptor and baroreceptor function in man', *New England Journal of Medicine* **282**(15), 823–829.